

P/Ca in Carbonates as a Proxy for Alkalinity and Phosphate Levels

**Miquela Ingalls^{1,†}, Clara L. Blättler², John A. Higgins³, John S. Magyar¹, John M. Eiler¹,
and Woodward W. Fischer¹**

¹Division of Geological and Planetary Sciences, California Institute of Technology, Pasadena, CA 91125 USA. ²Department of the Geophysical Sciences, The University of Chicago, Chicago, IL 60637 USA. ³Department of Geosciences, Princeton University, Princeton, NJ 08544 USA.

Corresponding author: Miquela Ingalls (ingalls@psu.edu)

†Current address: Department of Geosciences, The Pennsylvania State University, University Park, PA 16802, USA.

Key Points:

- Calcium-to-alkalinity ratios (Ca:ALK) in water determine rates and mechanisms of carbonate salt formation
- Shoreline tufa carbonate facies is a useful indicator of low Ca:ALK aqueous chemistry in the rock record
- Calcium isotope proxy for Ca:ALK in these materials is complicated by rate and mineralogical impacts on carbonate-water fractionation
- Carbonate P/Ca provides another means to assess Ca:ALK via the phosphate content of ancient aqueous environments

Abstract

Understanding mechanisms, rates, and drivers of past carbonate formation provides insight into the chemical evolution of Earth's oceans and atmosphere. We paired geological observations with elemental and isotope geochemistry to test potential proxies for calcium-to-alkalinity ratios (Ca:ALK). Across diverse carbonate facies from Pleistocene closed-basin lakes in Owens Valley, CA, we observed less $\delta^{44/40}\text{Ca}$ variation than theoretically predicted ($>0.75\%$) for the very low Ca:ALK in these systems. Carbonate clumped isotope disequilibria implied rapid carbonate growth—kinetic isotope effects, combined with the diverse carbonate minerals present, complicated the interpretation of $\delta^{44/40}\text{Ca}$ as a paleo-alkalinity proxy. In contrast, we observed that the high phosphate concentrations are recorded by shoreline and lake bottom carbonates formed in eleven Pleistocene lakes at orders of magnitude greater concentrations than in marine carbonates. Because the maximum phosphate content of water depends on Ca:ALK, we propose that carbonate P/Ca can inform phosphate levels and thereby Ca:ALK of aqueous environments in the carbonate record.

Plain Language Summary

Carbonate minerals record information about the local environments in which they form, for example along the margins of a lake or on the seabed, as well as the aqueous and atmospheric chemistry at the time of mineralization (e.g. pCO_2 , pH). This information is recorded in both the chemical signatures and textures carbonate rocks acquire during precipitation. Formation of calcium carbonate requires both a source of calcium (Ca^{2+}) and carbonate (CO_3^{2-} , or, carbonate alkalinity [ALK]). The ratio of calcium to alkalinity (Ca:ALK) in lake or ocean water influences carbonate saturation state, the rate of carbonate formation, the textures that carbonate will develop, and the chemical signatures recorded by the carbonate mineral. In this study, we tested several approaches to identify very low Ca:ALK chemistry in modern and ancient lakes. We found that water with extremely low levels of calcium and high levels of alkalinity forms carbonates with a characteristic “tufa” texture in stratigraphic positions tied to riverine and groundwater sources of Ca^{2+} . Moreover, the phosphate concentrations in these rocks were orders of magnitude higher than carbonates that precipitate under the high Ca:ALK conditions of modern oceans. Together the results illustrated that identification of carbonate tufa textures in the rock record and phosphate measurements of carbonate rocks can be used to study the ancient environments and mechanisms by which carbonate rocks formed.

1 Introduction

Geochemical signatures recorded by carbonate minerals are used to reconstruct ancient environmental and atmospheric conditions. However, the rates and mechanisms of carbonate formation, which are set by the geochemistry (and often biology) of the depositional environment, impact those materials. It is often challenging to determine the processes and environments responsible for carbonate precipitation in the geological record—particularly in strata devoid of fossils, as occurs in Precambrian sedimentary basins.

Broadly, carbonate formation is determined by a balance of cations (e.g. Ca^{2+} or Mg^{2+}) and the carbonate anion (CO_3^{2-}), which scales with carbonate alkalinity ($\text{ALK} = \text{HCO}_3^- + 2\text{CO}_3^{2-}$) in systems where pCO_2 is largely fixed and carbonate is the primary buffer, e.g. seawater and most lakes. Carbonate formation typically occurs between two end-member regimes: high alkalinity in

excess of Ca^{2+} ($\text{ALK} \gg \text{Ca}$, as in alkaline lakes), and vice versa (modern marine). Processes that source or consume cations (herein generalized as Ca^{2+}) and alkalinity set the carbonate saturation state of a solution ($\Omega = [\text{Ca}^{2+}][\text{ALK}]/K_{\text{sp}}^*$, where K_{sp}^* is the solubility product of CaCO_3 at a given temperature, pressure, and composition), and determine whether carbonate is likely to precipitate ($\Omega > 1$) or dissolve ($\Omega < 1$). The continuum of calcium-to-alkalinity ratios (Ca:ALK) that produce carbonate phases in natural environments varies by orders of magnitude. Where a given environment sits on that continuum impacts how carbonates get made.

Microbial metabolisms can contribute to carbonate formation and dissolution through the production and consumption of alkalinity and dissolved inorganic carbon (DIC; Vasconcelos & McKenzie, 1997; Folk & Chafetz, 2000). Photosynthesis and aerobic respiration increase and decrease Ω , respectively, by consuming and producing DIC (ΔDIC) with little to no change to ALK (ΔALK ; Bergmann et al., 2013; Higgins et al., 2009). The effect of these processes on Ω , however, depends on the Ca:ALK of the environment. In high Ca:ALK environments (modern marine Ca:ALK=4.1), Ω depends most on the production and consumption of DIC by microbial carbon cycling because Ca^{2+} is not limiting. In contrast, Ca^{2+} -starved, hyperalkaline environments, like Mono Lake, California (Ca:ALK=10⁻⁴), are less sensitive to localized ΔDIC because ΔALK is relatively insignificant compared to total ALK. Carbonate production from very low Ca:ALK water is controlled by processes that impact Ca^{2+} supply and cycling. For example, nearly all carbonate formed in Mono Lake and other alkaline, closed-basin Pleistocene lakes can be described as shoreline-proximal facies (e.g. tufa towers and shoreline crusts) wherein carbonate production is tied to external Ca^{2+} input from rivers and emergent groundwaters. In these settings, distal lake bottom sediments tend to be comparatively carbonate-poor. The shoreline-associated carbonate facies characteristic of low Ca:ALK systems can be useful geological indicators of this carbonate production regime, as long as they are preserved with sufficient stratigraphic and sedimentologic detail. However, diagnostic shoreline facies are rarely exposed in sedimentary basins. Due to the incompleteness of the record, we aimed to develop complementary geochemical proxies for Ca:ALK conditions that could be paired with field observations to assess paleo-alkalinity in ancient carbonate-producing systems.

1.1 Geochemical proxies for Ca:ALK in ancient environments

Based on a study of Ca isotope distillation in hyperalkaline Mono Lake (Nielsen & DePaolo 2013), Blättler and Higgins (2014) presented a framework in which Ca isotopes in evaporite salts could be used to reconstruct relative alkalinity. They found a notably large Ca isotope range ($\Delta\delta^{44/40}\text{Ca} > 1.5\text{‰}$) preserved within CaSO_4 salts in one evaporite system. From these measurements and experiments, they derived a relationship between $\Delta\delta^{44/40}\text{Ca}$ of evaporite minerals and cation-to-anion ratio of the aqueous solution to reconstruct $\text{Ca}^{2+}:\text{SO}_4^{2-}$ ratios in ancient evaporite sequences. By analogy to the Ca- SO_4 system and gypsum precipitation, Blättler et al. (2017) applied the same Ca isotope principles to evaluate how seawater carbonate chemistry might have changed over Earth history. Theoretically, when ALK greatly exceeds calcium concentration (Ca:ALK<0.75), like in Mono Lake, distillation driven by net evaporation should yield a $\Delta\delta^{44/40}\text{Ca} > 0.75\text{‰}$ within measurements from one evaporative carbonate sequence. The carbonate record, however, has additional mechanics that complicate $\Delta\delta^{44/40}\text{Ca}$ as a paleo-alkalinity proxy. First, evaporitic environments often precipitate multiple carbonate minerals (e.g. aragonite, vaterite, calcite, dolomite), and sometimes admixtures within co-occurring textures, each with unique Ca isotope fractionation factors (e.g. Gussone et al., 2005). Second, mechanisms and rates of carbonate precipitation are controlled by chemistry, hydrology, and biology in aqueous

systems. The rate of carbonate precipitation can change based on the relative contributions of these factors, thereby driving variable expression of kinetic isotope effects (KIEs) in calcium and other isotope systems in the resultant carbonate record.

There is a widely appreciated relationship between dissolved phosphate concentrations and DIC in modern alkaline lakes (e.g. Toner & Catling, 2020). In typical marine environments, phosphate abundance ($\leq 1 \mu\text{M}$ in surface waters) is set by biological consumption, organic matter decomposition, sedimentary burial and release of P scavenged by ferric iron oxides, and formation/dissolution of fluorapatite (Ruttenberg & Berner, 1993). With evolving atmospheric and oceanic redox chemistry and evolution of microfauna, marine P concentrations are thought to have fluctuated throughout Earth history, potentially to higher concentrations due to limited P scavenging under lower $p\text{O}_2$ conditions (e.g. Precambrian) or when expanses of deep ocean were anoxic (e.g. Cretaceous). However, phosphate concentrations can reach 100 mM in closed-basin lakes in quasistatic hydrological equilibrium (inflow approximately equal to evaporation).

Phosphate is typically a limiting nutrient due to biological uptake. However, the phosphate-concentrating mechanisms in alkaline lakewater greatly outpace biological consumption even in the extremely productive Mono Lake (10^9 - 10^{10} cells $\cdot\text{liter}^{-1}$ [Humayoun et al., 2003] versus surface seawater, $\sim 10^8$ cells $\cdot\text{liter}^{-1}$ [Whitman et al., 1998]). This is in part due to feedbacks on productivity by fixed nitrogen species which are often limiting in these systems (Herbst, 1998; Jellison & Melack, 2001). Further, in low Ca:ALK systems, Ca^{2+} is titrated by carbonate mineralization before low-solubility phosphate salts (e.g. apatite, vivianite) precipitate, which allows phosphate to accumulate in solution.

In this study, we hypothesized that phosphate should incorporate more-or-less proportional to its aqueous concentration in the carbonate phases precipitated from Mono, Searles, and other Pleistocene closed-basin lakes. We further proposed that carbonate P/Ca could be used to determine phosphate levels and relative alkalinity in the carbonate rock record.

2 Geologic setting, Samples and Methods

2.1 Field geology, facies descriptions, and mineralogy

Pleistocene Owens Valley, California, hosted a series of glacial lakes interconnected by the Owens River and fed by streams off of the Sierra Nevada range (Fig. 1). Today, these lakes exist either as restricted basins (e.g. Mono Lake) or as predominantly dry lake beds with seasonal wetting and drying (e.g. Searles Lake and Death Valley). The Searles dry lake bed and the relict shoreline facies of both Searles Lake and Pleistocene Lake Russell (proto-Mono Lake) are useful testing grounds for paleo-alkalinity proxies because they comprise geologically young carbonates

that have not yet been impacted by potential geochemical complications for which carbonate rocks are notoriously sensitive (i.e. burial-related heating or recrystallization).

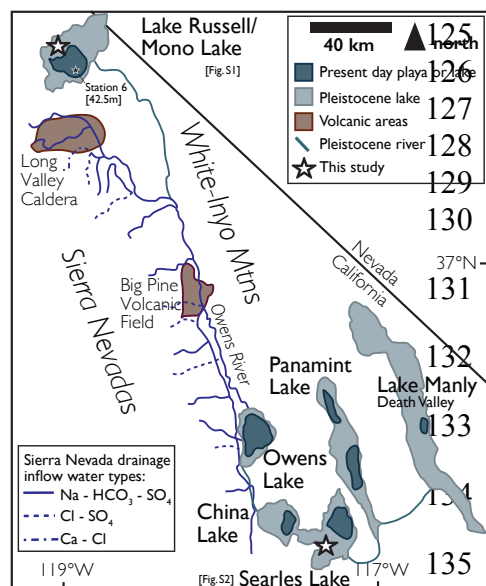


Figure 1. Interconnected alkaline lakes of Owens Valley, California, adapted from Smith (1979). The pale and dark teal shading marks the paleo- and modern shorelines, respectively. Line dashing denotes the water chemistry of the Sierran drainages that feed Owens River. Sampling sites are marked with stars.

Three field expeditions to Mono Lake and Searles Valley were conducted during 2019 (Figs. S1, S2; Table S1), during which diverse carbonate facies were collected (Fig. S3) and a stratigraphic section of the Pleistocene Wilson Creek Formation was measured (Fig. S4). During summer 2018, a one-meter sediment gravity core was collected in collaboration with the International Geobiology Course from Mono Lake at Station 6 (USGS), in the deepest part of the lake (42.5 m). This core contains sediment deposited over the past ~150 years, and was subsampled every 5 cm.

Carbonate mineralogy was determined by x-ray diffraction (XRD) at the California Institute of Technology (Text S1). An aragonite-calcite calibration curve (Fig. S5) was used to quantify samples of mixed mineralogy. Peak areas were integrated at 2θ of 25.6° to 26.7° for aragonite and 28.7° to 30.0° for calcite.

2.1 Calcium isotopes

Approximately 5 mg of bulk carbonate were processed for calcium isotope analysis following the methods of Blättler et al. (2018). Carbonate minerals were dissolved in 0.1N buffered acetic acid, and centrifuged to separate insoluble material. The resulting supernatant was diluted to approximately 30 ppm Ca^{2+} , and purified by ion chromatography using an automated Thermo-Dionex ICS-5000+ with a fraction collector. The purified calcium solutions were diluted in 2% nitric acid to a concentration of 2 ppm calcium for mass spectrometry (Text S2). Isotopic ratios of calcium were analyzed at Princeton University with a Thermo Neptune Plus multi-collector inductively coupled plasma mass spectrometer (ICP-MS) with an ESI Apex-IR sample introduction system. Corrections for mass interferences and standardization procedures are described in Text S2. $\delta^{44/42}\text{Ca}$ values were calculated relative to modern seawater by sample-standard bracketing. External precision on $\delta^{44/40}\text{Ca}$ values is $\pm 0.14\text{‰}$ (2σ), derived from the long-

term reproducibility of the carbonate standard SRM-915b treated as an unknown sample (n=199 from 2014 to 2018).

2.2 Clumped (Δ_{47}) isotopes

The carbonate clumped isotope thermometer is based on the energetics of “clumping” of the rare, heavy isotopes of carbon and oxygen (^{13}C and ^{18}O) at low temperatures (Eiler, 2007). This geothermometer relies on the measurement of the mass-47 anomaly (Δ_{47}) defined as the enrichment of the $^{13}\text{C}^{18}\text{O}^{16}\text{O}$ isotopologue of CO_2 relative to a stochastic distribution of the heavy isotopes among all CO_2 molecules: $\Delta_{47} = \left(\frac{^{47}\text{R}}{^{47}\text{R}^*} - 1 \right) \times 1000$ where $^{47}\text{R} = \frac{[^{13}\text{C}^{16}\text{O}^{18}\text{O} + ^{12}\text{C}^{17}\text{O}^{18}\text{O} + ^{13}\text{C}^{17}\text{O}_2]}{[^{12}\text{C}^{16}\text{O}_2]}$ and * denotes a stochastic intramolecular distribution of isotopes. Carbonate clumped isotope measurements were made at the California Institute of Technology over three analytical sessions from March 2019 to January 2020 (Table A3) following the analytical and data reduction procedures of Ingalls et al. (2020) (Text S3).

We used clumped isotopes in this study to investigate potential disequilibrium in carbonates forming rapidly in alkaline systems. Departures from carbonate clumped isotope equilibrium are most sensitive to parameters that impact the DIC composition (Watkins & Hunt, 2015). For example, experiments and natural samples have shown Δ_{47} depletions in carbonates formed from waters affected by HCO_3^- dehydration and dehydroxylation and Δ_{47} enrichments in carbonates affected by CO_2 hydration and hydroxylation (e.g., Saenger et al., 2012; Hill et al., 2014; Daeron et al., 2019), with a greater effect in high pH. Disequilibrium can also be driven by rapid carbonate precipitation rates because of the slow interconversion between CO_2 and HCO_3^- in the precipitating solution (Guo, 2020; Watkins & Hunt, 2015). Sample isotopic heterogeneity due to carbonate precipitating at a range of conditions that promote variable Δ_{47} disequilibrium can cause larger variance in replicate measurements and significant deviation in $T(\Delta_{47})$ from precipitation temperatures (Guo, 2020). Importantly, a carbonate system out of isotopic equilibrium with respect to one set of equilibria may also yield disequilibrium behavior in other isotope systems, e.g. Ca isotopes, and inform other geochemical data impacted by kinetics (e.g. Thiagarajan et al., 2020).

2.3 Phosphorus-to-calcium ratios

Phosphate concentrations were measured by the malachite green method (Ohno & Zibilske, 1991; Van Veldhoven & Mannaerts, 1987) colorimetric assay with a Biotek Cytation5 plate reader. Approximately 25 mg of carbonate powder was dissolved in 0.33 M acetic acid and ultrasonicated for >4 hours. A weak acid was chosen to avoid leaching of organic phosphorus and other phosphorus-bearing minerals like apatite. Three unique dilutions of each sample solution with three replicates of each dilution were pipetted into a well plate, for a total of at least nine absorbance readings per sample. An Abcam phosphate standard (ab65622) was used to generate calibration curves of 0 to 25 μM P for each plate. 30 μl of a proprietary formulation of malachite green and ammonium molybdate was added to each well and incubated in the dark for 30 minutes to facilitate the complexation of the heteropoly molybdophosphate that gives an absorption band

at a wavelength of 650 nm. The dissolved CaCO_3 mass, volume of solution, and nmol P measured by absorbance were used to calculate P/Ca molar ratios (Text S4).

3 Results and Discussion

3.1 Field observations to identify closed-basin chemistry without geochemical tools

In very low Ca:ALK systems, the loci of carbonate formation are almost entirely restricted to zones where Ca^{2+} -charged freshwater inputs mix with Ca^{2+} -starved and DIC-rich lake water. Tufa ‘towers’, ranging from meter- to tens of meters-scale (Fig. S3k), grew directly out of alluvial fan and deltaic deposits in the Wilson Creek Formation and at sites of spring discharge at both Mono and Searles (Fig. S3i).

Shoreline tufas were found draping igneous bedrock and volcanics at both sites (Fig. S3h)—these were generally more laterally extensive than the towers and, in places, exhibited reef-like morphologies. Tufa textures were subdivided into nodular, columnar or dendritic, and porous growth habits with fine laminations that could be identified on both the micro- and macroscopic scale. Tufas at both locations were variably cemented, and often encased in a laminated crust. These textures and their proposed formation mechanisms have been described elsewhere (e.g., Dunn, 1953; Guo & Chafetz, 2012).

Multiple tufa fabrics identified in this study can be morphologically linked to relatively rapid mineralization under low Ca:ALK conditions. We identified casts of brine fly pupae casings and tens-of-meters-scale reefs of carbonate-coated algal filaments (Fig. S3b). The *in vivo* preservation of fauna and cellular morphology by carbonate prior to decay indicated that precipitation occurred on biological rather than geological timescales.

Minimal carbonate precipitation occurs in the water column at Mono Lake. Most water column carbonate formation is thought to occur rapidly when the chemocline overturns and slightly Ca^{2+} -enriched, lower salinity, oxygenated surface water mixes with anoxic, alkaline bottom water to create transient $\Omega > 1$ conditions (Nielsen & DePaolo, 2013). The sediment core from Mono Lake was carbonate-poor and organic-rich (~5-10 wt.% total organic carbon; Fig. S3L). We hypothesized that the finely laminated muddy sediment should yield an organic-rich shale under compaction and diagenesis—a lithotype not typically targeted for study of ancient carbonates or for carbonate-based proxy materials, and thus, geochemical signals recorded in these sediments may be overlooked in geological studies. Finely laminated lake bottom sediments from both the Wilson Creek Formation and Searles were also carbonate-poor (Fig. S3g), suggesting that—as occurs today in Mono Lake—relatively little water column carbonate precipitation occurred in the Pleistocene lakes.

Slightly acidic closed-basin lakes, such as Andean Laguna Negra with Ca-Na-Cl water, can also form carbonate at shoreline freshwater-lakewater mixing zones. Laguna Negra’s Ω is limited by low pH rather than calcium. Carbonates described at Laguna Negra are morphologically and genetically associated with the microbial mats that form in mixing zones due to increased pH and reduced salinity (Gomez et al., 2014). Laguna Negra microbialites and oncoids form wrinkled and clotted textures in micritic to sparry laminae, which are easily differentiated from porous tufa fabrics. Thus, identification of tufa-like textures in stratigraphic positions that indicate riverine and groundwater inputs (e.g. on fans, within deltas, or near shorelines) can be used to help identify low Ca:ALK systems in the record. However, chemical proxies are necessary to quantitatively estimate Ca:ALK in geological systems with insufficient preservation or outcrop exposure.

3.2 Ca isotope range as a proxy for Ca:ALK

The magnitude of calcium isotope fractionation between a carbonate mineral and water is determined by mineralogy, precipitation rate, and the Ca:ALK of the solution. When $\text{Ca:ALK} < 0.75$, dissolved Ca^{2+} is near-quantitatively removed by carbonate formation during evaporitic concentration of solutes, yielding $>0.75\%$ of Ca distillation and, thus, $\Delta\delta^{44/40}\text{Ca}_{\text{water}}$ (Fig. 2a; Nielsen & DePaolo, 2013). To test if the predicted $\Delta\delta^{44/40}\text{Ca}$ could be recovered in evaporitic carbonate salts that formed in the Pleistocene Owens Valley lake systems, we measured the carbonate facies found in modern Mono Lake and Pleistocene Lakes Russell (Wilson Creek Formation) and Searles, which presumably precipitated from similarly low Ca:ALK waters. However, our $\delta^{44/40}\text{Ca}_{\text{carb}}$ measurements yielded total ranges of 0.68% and 0.52% from Pleistocene Lakes Russell and Searles, respectively—values below the 0.75% threshold expected for low Ca:ALK systems (Fig. 2b). The diverse carbonates sampled in this study did not capture the anticipated isotopic distillation behavior.

Carbonate precipitated within the water column of the most open part of the lake where Ca^{2+} is lowest, and evaporative concentration of Ca^{2+} is necessary for mineralization, should yield the greatest isotopic distillation. As such, we predicted we would measure $>0.75\%$ $\Delta\delta^{44/40}\text{Ca}$ driven by evaporative precipitation from the Mono Lake sediment core. Subsamples were collected every 5 cm to simulate relatively fine sampling practices for very fine-scaled chemostratigraphy with the goal of detecting chemical perturbations. However, we found a range of $\delta^{44/40}\text{Ca}$ of 0.47% within the core. A finer-scale sampling and/or analytical technique may be required to resolve evaporative distillation events.

We can better predict and identify Rayleigh behavior in a system that precipitates the full evaporite mineral sequence (i.e., carbonate, gypsum, halite). However, Mono Lake is undersaturated with respect to gypsum, and thus, only accumulates carbonate salts. In the absence of other evaporite minerals, it is difficult to identify evaporative versus equilibrium precipitation. Because we were unable to recover the modeled $\Delta\delta^{44/40}\text{Ca}$ within a diverse range of carbonate facies in modern sediments prior to diagenetic modification, it may be exceedingly difficult to recover Rayleigh distillation of Ca isotopes in ancient lacustrine sediments. While the perfect stratigraphic section preserving multiple evaporitic carbonate sequences might exist, the difficulty of recovering such sequences in modern and recent settings where we have absolute constraints on Ca:ALK suggested that Ca isotope range may be better interpreted when employed concurrently with an additional tool for reconstructing Ca:ALK.

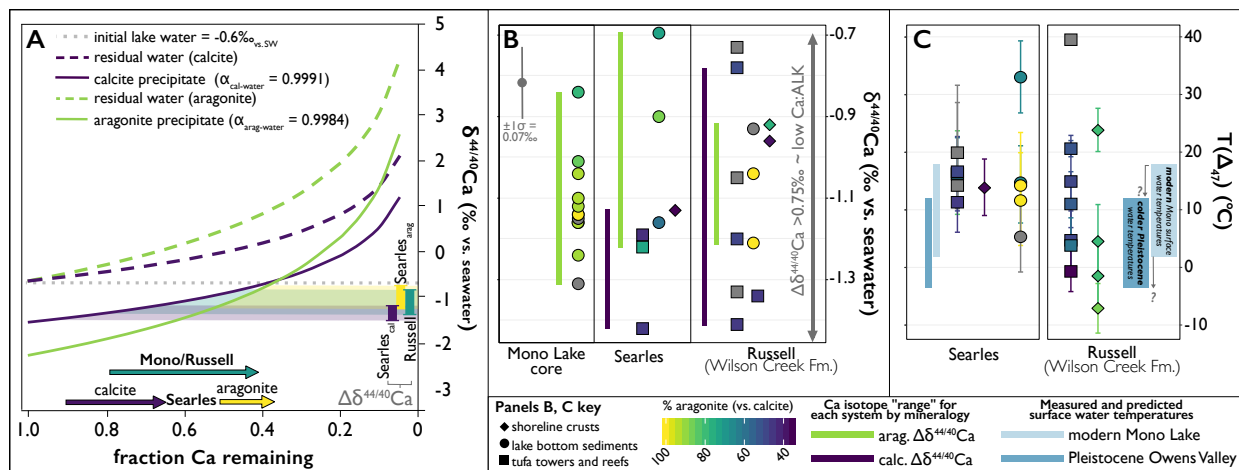


Figure 2. Stable isotope effects of low Ca:ALK water. (a) Expected Rayleigh distillation of Ca isotopes during evaporative precipitation of aragonite (green) and calcite (purple). Vertical bars plot $\delta^{44/40}\text{Ca}$ ranges from Searles calcite and aragonite, and the Mono-Russell system. Ca ranges were projected to the mineral-specific Rayleigh curves to determine the fraction of Ca removed during evaporative mineral precipitation (arrows), or degree of distillation under model assumptions. The starting $\delta^{44/40}\text{Ca}_{\text{water}}$ of -0.6‰ is 0.1‰ higher than the most distilled Mono Lake water reported in Nielsen & DePaolo (2013) and the upper limit of the $\delta^{44/40}\text{Ca}$ value of water that could precipitate our lowest calcite $\delta^{44/40}\text{Ca}$ values. (b) Ca isotope data from a modern Mono Lake core and Pleistocene Lakes Russell and Searles. The gray arrow marks the theoretically predicted range evaporative precipitation from low Ca:ALK water should exceed. Points in panels B and C are colored by percent aragonite. Green and purple bars mark $\Delta\delta^{44/40}\text{Ca}$ binned by aragonite ($>60\%$) or calcite, respectively. (c) Large intra- (error bars) and intersample carbonate clumped isotope variability, as well as $T(\Delta_{47})$ exceeding the modern annual range of Mono Lake surface water temperatures (light blue box) and predicted cooler Pleistocene temperatures in Owens Valley (teal), suggests Δ_{47} disequilibrium.

Variable mineralogy and precipitation kinetics tend to expand the total $\Delta\delta^{44/40}\text{Ca}$ beyond the range driven by Rayleigh distillation. First, aragonite and calcite have different $^{44/40}\text{Ca}$ $\alpha_{\text{carb-water}}$ fractionation factors (Gussone et al., 2005). Each carbonate phase that precipitates from the same $\delta^{44/40}\text{Ca}_{\text{water}}$ yields different $\delta^{44/40}\text{Ca}_{\text{carb}}$ values (Fig. 2a). This is important when considering an ancient carbonate system that may have formed as a mixed-mineral assemblage but has been diagenetically replaced by calcite and/or dolomite; a large $\Delta\delta^{44/40}\text{Ca}$ value resulting from different mineralogical fractionations could be misinterpreted as evaporative distillation. In Mono and Searles Lakes, we identified both aragonite and calcite with pseudomorphic textures of primary cold-water carbonates, ikaite and monohydrated calcite (Fig. S3e). We considered $\Delta\delta^{44/40}\text{Ca}$ of each carbonate phase separately to avoid confounding mineralogical and distillation effects. The Mono-Russell system had a $\Delta\delta^{44/40}\text{Ca}_{\text{cal}}$ of 0.56‰ and $\Delta\delta^{44/40}\text{Ca}_{\text{arag}}$ of 0.47‰ . Searles Lake yielded $\Delta\delta^{44/40}\text{Ca}_{\text{cal}}$ of 0.32‰ and $\Delta\delta^{44/40}\text{Ca}_{\text{arag}}$ of 0.53‰ .

Additionally, we suspected that some amount of $\Delta\delta^{44/40}\text{Ca}$ could be explained by varying KIEs—driven by differences in carbonate precipitation rates between fabrics, and between individual tufa samples (Lemarchand et al., 2004). Tufas from the Wilson Creek Formation (Russell), and Mono and Searles Lakes yielded $T(\Delta_{47})$ values ranging from $-7.1\pm 4.3^{\circ}\text{C}$ to $39.5\pm 4.5^{\circ}\text{C}$ (Fig. 2; Table A2). This amount of $T(\Delta_{47})$ variability is geologically implausible, both within individual samples (i.e. large error bars capture variability in measurements from the same tufa) and between tufas formed within each basin under similar climate conditions. Furthermore, Owens Valley tufas have never experienced high-temperature burial or hydrothermal alteration, which drives $T(\Delta_{47})$ to higher apparent temperatures. Some of the tufas yield warmer apparent temperatures than modern summertime (JJA) surface water temperatures (Schneider et al., 2009; Fig. 2). Additionally, we anticipated that carbonates formed during the Pleistocene glacial periods should have yielded colder formation temperatures than modern. We attributed the unusually warm $T(\Delta_{47})$ values and sample heterogeneity to variably expressed KIEs driven by fast tufa carbonate formation. Although magnitude of KIEs are independent, both Δ_{47} and Ca isotopes are susceptible to precipitation rate-driven KIEs (Thiagarajan et al., 2020), and thus we hypothesized that some amount of the tufa $\delta^{44/40}\text{Ca}$ variability captured kinetics in ways that masked the expected patterns of Rayleigh distillation.

3.3 High P/Ca in carbonates formed from low Ca:ALK water

Carbonates that formed within modern Mono Lake, Pleistocene Lakes Russell and Searles, and other Pleistocene lakes yielded P/Ca ratios up to three orders of magnitude greater than marine carbonate (Fig. 3). All carbonate facies from Searles Lake displayed P/Ca values from 0.432 ± 0.019 to 3.177 ± 0.177 mmol/mol. Carbonates from the one-meter Mono Lake core ranged from 0.674 ± 0.033 to 1.301 ± 0.112 mmol/mol. The highest P/Ca values were from the Pleistocene Wilson Creek Formation, which ranged from 1.192 ± 0.082 to 13.995 ± 0.794 mmol/mol. Carbonate pebble coatings from a lag pavement in a deltaic fan at the base of the Wilson Creek Formation yielded 3.209 mmol P/mol Ca. From sedimentological observations, we interpreted that these coated clasts formed in the wave spray/swash zone during early lake-level rise when the lake was still undergoing cycles of wetting and drying typical of very shallow, saline lakes. Given these values, Lake Russell may have had a low Ca:ALK early when lake levels were still low and dissolved solute levels were highly sensitive to evaporation.

In marine materials, the majority of existing P/Ca data were derived from coral skeletons (Anagnostou et al., 2011; Chen et al., 2019), with the highest P/Ca concentrations in deep-water species *D. dianthus*. Chen et al. (2019) showed that P was incorporated into coral aragonite in proportion to its concentration in surrounding seawater. Biogenic coral aragonite populated the lowest mode of P/Ca, ranging from 0.003 to 0.118 mmol/mol—lower values than biogenic calcite or abiotic marine aragonite and calcite (Fig. S6). Aragonitic, calcitic, and dolomitic marine cements and ooids and biogenic calcite comprised the second lowest P/Ca mode from 0.049 to 0.184 mmol/mol (Fig. 3a, S6). There was no statistical difference between biogenic calcite and abiotic marine carbonate P/Ca, which was interpreted as phosphate partitioning without strong dependencies on biogenicity and carbonate mineralogy.

Marine carbonates and those from Pleistocene to modern alkaline lakes formed distinct P/Ca populations with minimal overlap (Fig. 3a). The minor overlap seen between marine and nonmarine carbonate data could be due to the complexities of impurity incorporation into carbonate minerals (Gutjahr et al., 1996; Nielsen et al., 2013) as well as natural variability in both dissolved phosphate concentrations and Ca:ALK in both marine and terrestrial systems. Nonetheless, the striking bimodality of the P/Ca data between high and low Ca:ALK systems presented a means by which to differentiate between end-member chemical environments (Fig. 3a).

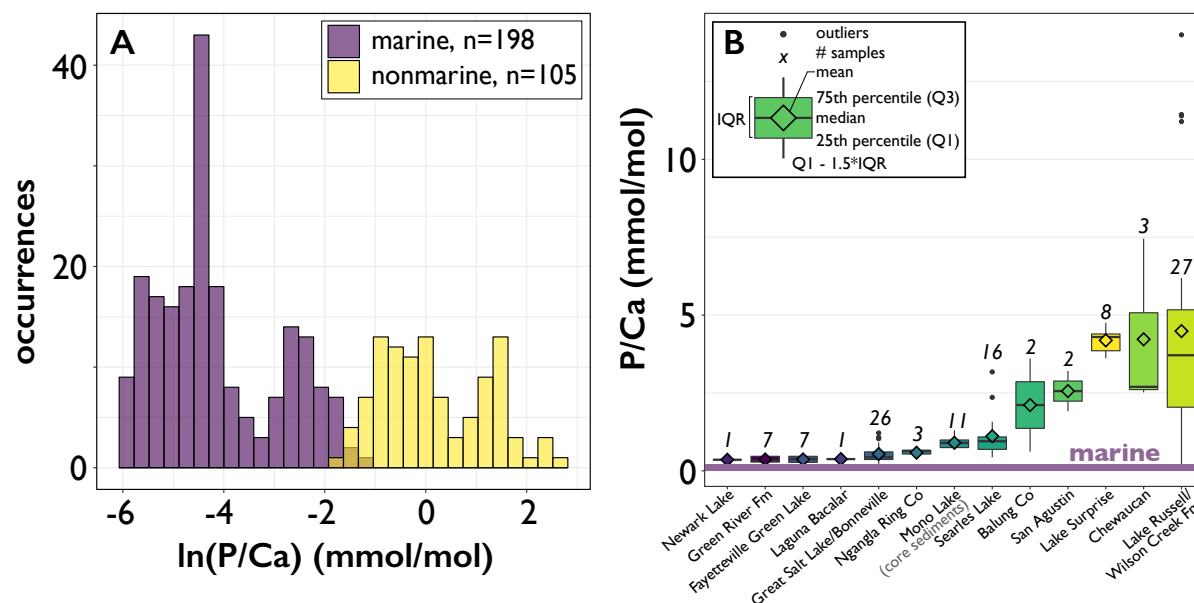


Figure 3. Phosphorus-to-calcium ratios of marine and closed-basin lake carbonates. (a) Distribution of marine (purple) and nonmarine (yellow) carbonate P/Ca measured in this study and some marine measurements using the same method in the literature (Anagnostou et al., 2011; Chen et al., 2019). (b) Nearly all carbonate P/Ca from restricted basins are substantially greater than marine values.

We assessed if phosphate enrichments in Owens Valley lacustrine carbonates were more related to chemical weathering of Sierran bedrock specifically, rather than Ca:ALK, by analyzing shoreline tufa from 10 sites with idiosyncratic basin geology (Table A1): the Eocene Green River Formation and Pleistocene to modern lake basins from Tibet and western North America (Fig. 3). All tufa P/Ca ratios were highly elevated above median marine values. The mean P/Ca values from Balung Co, San Agustin, Lake Surprise, and Lake Chewaucan were comparable with the extreme P/Ca values from Owens Valley, demonstrating that the extremely high phosphate levels found in Mono Lake water and partitioned into tufa carbonate are non-unique and shoreline tufa facies can be a meaningful indicator of elevated phosphate levels and possibly low Ca:ALK chemistry in the carbonate record.

Elevated P/Ca values of 0.211 ± 0.027 to 0.533 ± 0.094 mmol/mol observed in seven tufas, stromatolites, and cements from the Eocene Green River Formation demonstrated that carbonate-associated phosphate enrichments could be preserved through burial diagenesis. It remains to be tested how robust this P/Ca signal is in deeper time, but we have seen that the high phosphate levels that are correlated with Ca:ALK in these systems can be captured in the carbonate minerals they produce.

4 Conclusions

The ability to reconstruct alkalinity at specific times and basins in Earth's past allows us to better understand the processes responsible for the generation of the carbonate record, and evaluate secular changes in seawater chemistry over Earth history. Geological observations of textures, fabrics, facies, and stratal geometry of carbonate-rich units provide useful constraints on ancient

Ca:ALK based on characteristic modes of carbonate formation in low or high Ca:ALK systems. In the Pleistocene lake system of Owens Valley, we found that carbonate formation is tied closely to processes that add Ca^{2+} to the water, as compared to high Ca:ALK systems (e.g. marine basins), wherein carbonate formation is more tied to biogeochemical processes that impact the distribution of DIC and alkalinity. We also examined potential geochemical proxies for reconstructing Ca:ALK. Ca-isotope range has previously been used to reconstruct Ca:ALK of ancient environments based on Rayleigh distillation behavior within the Ca^{2+} -starved water column of Mono Lake. However, we were unable to recover the theoretically predicted $> 0.75\%$ range from carbonates formed in Ca^{2+} -starved waters in Mono, Russell, and Searles Lakes. We hypothesized that mineralogical differences (i.e. aragonite vs. calcite) and rate dependence of $\alpha_{\text{carb-water}}$ complicated interpretations of $\Delta\delta^{44/40}\text{Ca}$ in the diverse carbonate phases that form in these hyperalkaline lake systems. An unreasonable range of $T(\Delta_{47})$ values within individual samples and between samples from the same basin, as well as much warmer temperatures than expected from carbonates that precipitated during glacial periods, supported the view that isotopic disequilibrium and precipitation kinetics are important in these systems.

Based on our understanding of the mechanics that lead to high phosphate concentrations in alkaline systems, we studied carbonate-associated P/Ca as a potential proxy for the phosphate content and Ca:ALK in ancient aqueous environments. Carbonates that formed in closed-basin lakes under Ca^{2+} -starved conditions yielded orders of magnitude greater P/Ca ratios than modern and ancient marine carbonate. Phosphate was incorporated into carbonates relatively proportional to the Ca:ALK of the system. Questions remain about how robust P/Ca is to post-depositional processes that impact the geochemistry of ancient carbonates. However, we found that P/Ca was robust through burial diagenesis and partial silicification of carbonates in the Eocene Green River Formation, and posited that—along with geological constraints—P/Ca has the potential to be useful in identifying phosphate levels and Ca:ALK in ancient environments.

Acknowledgments, Samples, and Data

Supporting information detailing methods and all data may be found in the Supplemental Information, and were archived in the Open Science Framework (doi: 10.17605/OSF.iO/N9Y3H). Samples collected as a part of this study were registered with IGSNs, listed in Table S1. The authors would like to thank Christine Chen, Adam Hudson, Dan Ibarra, Max Lloyd and Theodore Present for contributing sample material from other paleo-lakes and marine carbonates, and the International Geobiology Course (supported by the Agouron Institute, Simons Foundation, NASA, and Caltech) for access to Mono Lake sediment cores. Funding for the work was provided by the Simons Foundation Collaboration on the Origins of Life (WWF) and Barr Foundation Postdoctoral Fellowship to MI.

References

Anagnostou, E., Sherrell, R. M., Gagnon, A., LaVigne, M., Field, M. P., & McDonough, W. F. (2011). Seawater nutrient and carbonate ion concentrations recorded as P/Ca, Ba/Ca, and U/Ca in the deep-sea coral *Desmophyllum dianthus*. *Geochimica et Cosmochimica Acta*, 75(9), 2529–2543. <https://doi.org/10.1016/j.gca.2011.02.019>

- 420 Bergmann, K. D., Grotzinger, J. P., & Fischer, W. W. (2013). Biological Influences on Seafloor
421 Carbonate Precipitation. *Palaaios*, 28(2), 99–115. [https://doi.org/10.2110/palo.2012.p12-](https://doi.org/10.2110/palo.2012.p12-088r)
422 088r
- 423 Blättler, C. L., Kump, L. R., Fischer, W. W., Paris, G., Kasbohm, J. J., & Higgins, J. A. (2017).
424 Constraints on ocean carbonate chemistry and pCO₂ in the Archaean and
425 Palaeoproterozoic. *Nature Geoscience*, 10(1), 41–45. <https://doi.org/10.1038/ngeo2844>
- 426 Blättler, C. L., Claire, M. W., Prave, A. R., Kirsimäe, K., Higgins, J. A., Medvedev, P. V., et al.
427 (2018). Two-billion-year-old evaporites capture Earth’s great oxidation. *Science*,
428 360(6386), 320–323. <https://doi.org/10.1126/science.aar2687>
- 429 Blättler, Clara L., & Higgins, J. A. (2014). Calcium isotopes in evaporites record variations in
430 Phanerozoic seawater SO₄ and Ca. *Geology*, 42(8), 711–714.
431 <https://doi.org/10.1130/G35721.1>
- 432 Chen, M., Martin, P., Goodkin, N. F., Tanzil, J., Murty, S., & Wiguna, A. A. (2019). An
433 assessment of P speciation and P:Ca proxy calibration in coral cores from Singapore and
434 Bali. *Geochimica et Cosmochimica Acta*, 267, 113–123.
435 <https://doi.org/10.1016/j.gca.2019.09.024>
- 436 Daeron, M., Drysdale, R. N., Peral, M., Huyghe, D., Blamart, D., Coplen, T. B., et al. (2019).
437 Most Earth-surface calcites precipitate out of isotopic equilibrium. *Nature Communications*,
438 10(1), 1–7. <https://doi.org/10.1038/s41467-019-08336-5>
- 439 Dunn, J. R. (1953). The origin of the deposits of tufa in Mono Lake [California]. *Journal of*
440 *Sedimentary Research*. <https://doi.org/10.1306/d4269530-2b26-11d7-8648000102c1865d>
- 441 Eiler, J. M. (2007). “Clumped-isotope” geochemistry—The study of naturally-occurring,
442 multiply-substituted isotopologues. *Earth and Planetary Science Letters*, 262(3–4), 309–
443 327. <https://doi.org/10.1016/j.epsl.2007.08.020>
- 444 Folk, R. L., & Chafetz, H. S. (2000). Bacterially Induced Microscale and Nanoscale Carbonate
445 Precipitates. In *Microbial Sediments*. https://doi.org/10.1007/978-3-662-04036-2_6
- 446 Gomez, F. J., Kah, L. C., Bartley, J. K., & Astini, R. A. (2014). Microbialites in a High-Altitude
447 Andean Lake: Multiple Controls on Carbonate Precipitation and Lamina Accretion. *Palaaios*,
448 29(6), 233–249. <https://doi.org/10.2110/palo.2013.049>
- 449 Guo, W. (2020). Kinetic Clumped Isotope Fractionation in the DIC-H₂O-CO₂ System: Patterns,
450 Controls and Implications. *Geochimica et Cosmochimica Acta*, 268, 230–257.
451 <https://doi.org/https://doi.org/10.1016/j.gca.2019.07.055>
- 452 Guo, X., & Chafetz, H. S. (2012). Large tufa mounds, Searles Lake, California. *Sedimentology*,
453 59(5), 1509–1535. <https://doi.org/10.1111/j.1365-3091.2011.01315.x>
- 454 Gussone, N., Böhm, F., Eisenhauer, A., Dietzel, M., Heuser, A., Teichert, B. M. A., et al. (2005).
455 Calcium isotope fractionation in calcite and aragonite. *Geochimica et Cosmochimica Acta*,

- 456 69(18), 4485–4494. <https://doi.org/10.1016/j.gca.2005.06.003>
- 457 Gutjahr, A., Dabringhaus, H., & Lacmann, R. (1996). Studies of the growth and dissolution
458 kinetics of the CaCo₃ polymorphs calcite and aragonite II. The influence of divalent cation
459 additives on the growth and dissolution rates. *Journal of Crystal Growth*.
460 [https://doi.org/10.1016/0022-0248\(95\)00447-5](https://doi.org/10.1016/0022-0248(95)00447-5)
- 461 Herbst, D. B. (1998). Potential salinity limitations on nitrogen fixation in sediments from Mono
462 Lake, California. *International Journal of Salt Lake Research*.
463 <https://doi.org/10.1023/A:1009001514449>
- 464 Higgins, J. A., Fischer, W. W., & Schrag, D. P. (2009). Oxygenation of the ocean and sediments:
465 Consequences for the seafloor carbonate factory. *Earth and Planetary Science Letters*,
466 284(1–2), 25–33. <https://doi.org/10.1016/j.epsl.2009.03.039>
- 467 Hill, P. S., Tripathi, A. K., & Schauble, E. A. (2014). Theoretical constraints on the effects of pH,
468 salinity, and temperature on clumped isotope signatures of dissolved inorganic carbon
469 species and precipitating carbonate minerals. *Geochimica et Cosmochimica Acta*, 125, 610–
470 652. <https://doi.org/10.1016/j.gca.2013.06.018>
- 471 Humayoun, S. B., Bano, N., & Hollibaugh, J. T. (2003). Depth distribution of microbial diversity
472 in Mono Lake, a meromictic soda lake in California. *Applied and Environmental*
473 *Microbiology*, 69(2), 1030–1042. <https://doi.org/10.1128/AEM.69.2.1030>
- 474 Ingalls, M., Frantz, C. M., Snell, K. E., & Trower, E. J. (2020). Carbonate facies-specific stable
475 isotope data record climate, hydrology, and microbial communities in Great Salt Lake, UT.
476 *Geobiology*, 28. <https://doi.org/10.1111/gbi.12386>
- 477 Jellison, R., & Melack, J. M. (2001). Nitrogen limitation and particulate elemental ratios of
478 seston in hypersaline Mono Lake, California, U.S.A. In *Saline Lakes*. Springer.
479 https://doi.org/10.1007/978-94-017-2934-5_1
- 480 Lemarchand, D., Wasserburg, G. J., & Papanastassiou, D. A. (2004). Rate-controlled calcium
481 isotope fractionation in synthetic calcite. *Geochimica et Cosmochimica Acta*, 68(22), 4665–
482 4678. <https://doi.org/10.1016/j.gca.2004.05.029>
- 483 Nielsen, L. C., & DePaolo, D. J. (2013). Ca isotope fractionation in a high-alkalinity lake
484 system: Mono Lake, California. *Geochimica et Cosmochimica Acta*, 118, 276–294.
485 <https://doi.org/10.1016/j.gca.2013.05.007>
- 486 Nielsen, L. C., De Yoreo, J. J., & DePaolo, D. J. (2013). General model for calcite growth
487 kinetics in the presence of impurity ions. *Geochimica et Cosmochimica Acta*, 115, 100–114.
488 <https://doi.org/10.1016/j.gca.2013.04.001>
- 489 Ohno, T., & Zibilske, L. M. (1991). Determination of low concentrations of phosphorus in soil
490 extracts using malachite green. *Soil Science Society of America Journal*.
491 <https://doi.org/10.2136/sssaj1991.03615995005500030046x>

- 492 Ruttenberg, K. C., & Berner, R. A. (1993). Authigenic apatite formation and burial in sediments
493 from non-upwelling, continental margin environments. *Geochimica et Cosmochimica Acta*,
494 57(5), 991–1007. [https://doi.org/10.1016/0016-7037\(93\)90035-U](https://doi.org/10.1016/0016-7037(93)90035-U)
- 495 Saenger, C., Affek, H. P., Felis, T., Thiagarajan, N., Lough, J. M., & Holcomb, M. (2012).
496 Carbonate clumped isotope variability in shallow water corals: Temperature dependence
497 and growth-related vital effects. *Geochimica et Cosmochimica Acta*, 99, 224–242.
498 <https://doi.org/10.1016/j.gca.2012.09.035>
- 499 Schneider, P., Hook, S. J., Radocinski, R. G., Corlett, G. K., Hulley, G. C., Schladow, S. G., &
500 Steissberg, T. E. (2009). Satellite observations indicate rapid warming trend for lakes in
501 California and Nevada. *Geophysical Research Letters*, 36(22), 1–6.
502 <https://doi.org/10.1029/2009GL040846>
- 503 Smith, G. I. (1979). Subsurface stratigraphy and geochemistry of Late Quaternary evaporites,
504 Searles Lake, California. *US Geological Survey, Professional Paper*, 1043, 130.
- 505 Spooner, P. T., Guo, W., Robinson, L. F., Thiagarajan, N., Hendry, K. R., Rosenheim, B. E., &
506 Leng, M. J. (2016). Clumped isotope composition of cold-water corals: A role for vital
507 effects? *Geochimica et Cosmochimica Acta*, 179, 123–141.
508 <https://doi.org/10.1016/j.gca.2016.01.023>
- 509 Thiagarajan, N., Crémière, A., Blättler, C., Lepland, A., Kirsimäe, K., Higgins, J., et al. (2020).
510 Stable and clumped isotope characterization of authigenic carbonates in methane cold seep
511 environments. *Geochimica et Cosmochimica Acta*, 279, 204–219.
512 <https://doi.org/10.1016/j.gca.2020.03.015>
- 513 Toner, J. D., & Catling, D. C. (2020). A carbonate-rich lake solution to the phosphate problem of
514 the origin of life. *Proceedings of the National Academy of Sciences of the United States of*
515 *America*, 117(2), 883–888. <https://doi.org/10.1073/pnas.1916109117>
- 516 Vasconcelos, C., & McKenzie, J. A. (1997). Microbial Mediation of Modern Dolomite
517 Precipitation and Diagenesis Under Anoxic Conditions (Lagoa Vermelha, Rio de Janeiro,
518 Brazil). *Journal of Sedimentary Research*. [https://doi.org/10.1306/D4268577-2B26-11D7-](https://doi.org/10.1306/D4268577-2B26-11D7-8648000102C1865D)
519 [8648000102C1865D](https://doi.org/10.1306/D4268577-2B26-11D7-8648000102C1865D)
- 520 Van Veldhoven, P. P., & Mannaerts, G. P. (1987). Inorganic and organic phosphate
521 measurements in the nanomolar range. *Analytical Biochemistry*.
522 [https://doi.org/10.1016/0003-2697\(87\)90649-X](https://doi.org/10.1016/0003-2697(87)90649-X)
- 523 Watkins, J. M., & Hunt, J. D. (2015). A process-based model for non-equilibrium clumped
524 isotope effects in carbonates. *Earth and Planetary Science Letters*, 432.
525 <https://doi.org/10.1016/j.epsl.2015.09.042>
- 526 Whitman, W. B., Coleman, D. C., & Wiebe, W. J. (1998). Prokaryotes: The unseen majority.
527 *Proceedings of the National Academy of Sciences of the United States of America*.
528 <https://doi.org/10.1073/pnas.95.12.6578>

Supplemental References

- Anagnostou, E., Sherrell, R. M., Gagnon, A., LaVigne, M., Field, M. P., & McDonough, W. F. (2011). Seawater nutrient and carbonate ion concentrations recorded as P/Ca, Ba/Ca, and U/Ca in the deep-sea coral *Desmophyllum dianthus*. *Geochimica et Cosmochimica Acta*, 75(9), 2529–2543. <https://doi.org/10.1016/j.gca.2011.02.019>
- Bergmann, K. D., Grotzinger, J. P., & Fischer, W. W. (2013). Biological Influences on Seafloor Carbonate Precipitation. *Palaaios*, 28(2), 99–115. <https://doi.org/10.2110/palo.2012.p12-088r>
- Blättler, C. L., Kump, L. R., Fischer, W. W., Paris, G., Kasbohm, J. J., & Higgins, J. A. (2017). Constraints on ocean carbonate chemistry and pCO₂ in the Archaean and Palaeoproterozoic. *Nature Geoscience*, 10(1), 41–45. <https://doi.org/10.1038/ngeo2844>
- Blättler, C. L., Claire, M. W., Prave, A. R., Kirsimäe, K., Higgins, J. A., Medvedev, P. V., et al. (2018). Two-billion-year-old evaporites capture Earth's great oxidation. *Science*, 360(6386), 320–323. <https://doi.org/10.1126/science.aar2687>
- Blättler, Clara L., & Higgins, J. A. (2014). Calcium isotopes in evaporites record variations in Phanerozoic seawater SO₄ and Ca. *Geology*, 42(8), 711–714. <https://doi.org/10.1130/G35721.1>
- Chen, M., Martin, P., Goodkin, N. F., Tanzil, J., Murty, S., & Wiguna, A. A. (2019). An assessment of P speciation and P:Ca proxy calibration in coral cores from Singapore and Bali. *Geochimica et Cosmochimica Acta*, 267, 113–123. <https://doi.org/10.1016/j.gca.2019.09.024>
- Daeron, M., Drysdale, R. N., Peral, M., Huyghe, D., Blamart, D., Coplen, T. B., et al. (2019). Most Earth-surface calcites precipitate out of isotopic equilibrium. *Nature Communications*, 10(1), 1–7. <https://doi.org/10.1038/s41467-019-08336-5>
- Dunn, J. R. (1953). The origin of the deposits of tufa in Mono Lake [California]. *Journal of Sedimentary Research*. <https://doi.org/10.1306/d4269530-2b26-11d7-8648000102c1865d>
- Eiler, J. M. (2007). “Clumped-isotope” geochemistry—The study of naturally-occurring, multiply-substituted isotopologues. *Earth and Planetary Science Letters*, 262(3–4), 309–327. <https://doi.org/10.1016/j.epsl.2007.08.020>
- Folk, R. L., & Chafetz, H. S. (2000). Bacterially Induced Microscale and Nanoscale Carbonate Precipitates. In *Microbial Sediments*. https://doi.org/10.1007/978-3-662-04036-2_6
- Gomez, F. J., Kah, L. C., Bartley, J. K., & Astini, R. A. (2014). Microbialites in a High-Altitude Andean Lake: Multiple Controls on Carbonate Precipitation and Lamina Accretion. *Palaaios*, 29(6), 233–249. <https://doi.org/10.2110/palo.2013.049>
- Guo, W. (2020). Kinetic Clumped Isotope Fractionation in the DIC-H₂O-CO₂ System: Patterns, Controls and Implications. *Geochimica et Cosmochimica Acta*, 268, 230–257. <https://doi.org/https://doi.org/10.1016/j.gca.2019.07.055>
- Guo, X., & Chafetz, H. S. (2012). Large tufa mounds, Searles Lake, California. *Sedimentology*, 59(5), 1509–1535. <https://doi.org/10.1111/j.1365-3091.2011.01315.x>
- Gussone, N., Böhm, F., Eisenhauer, A., Dietzel, M., Heuser, A., Teichert, B. M. A., et al. (2005). Calcium isotope fractionation in calcite and aragonite. *Geochimica et Cosmochimica Acta*, 69(18), 4485–4494. <https://doi.org/10.1016/j.gca.2005.06.003>
- Gutjahr, A., Dabringhaus, H., & Lacmann, R. (1996). Studies of the growth and dissolution kinetics of the CaCO₃ polymorphs calcite and aragonite II. The influence of divalent cation

- additives on the growth and dissolution rates. *Journal of Crystal Growth*.
[https://doi.org/10.1016/0022-0248\(95\)00447-5](https://doi.org/10.1016/0022-0248(95)00447-5)
- Herbst, D. B. (1998). Potential salinity limitations on nitrogen fixation in sediments from Mono Lake, California. *International Journal of Salt Lake Research*.
<https://doi.org/10.1023/A:1009001514449>
- Higgins, J. A., Fischer, W. W., & Schrag, D. P. (2009). Oxygenation of the ocean and sediments: Consequences for the seafloor carbonate factory. *Earth and Planetary Science Letters*, 284(1–2), 25–33. <https://doi.org/10.1016/j.epsl.2009.03.039>
- Hill, P. S., Tripathi, A. K., & Schauble, E. A. (2014). Theoretical constraints on the effects of pH, salinity, and temperature on clumped isotope signatures of dissolved inorganic carbon species and precipitating carbonate minerals. *Geochimica et Cosmochimica Acta*, 125, 610–652. <https://doi.org/10.1016/j.gca.2013.06.018>
- Humayoun, S. B., Bano, N., & Hollibaugh, J. T. (2003). Depth distribution of microbial diversity in Mono Lake, a meromictic soda lake in California. *Applied and Environmental Microbiology*, 69(2), 1030–1042. <https://doi.org/10.1128/AEM.69.2.1030>
- Ingalls, M., Frantz, C. M., Snell, K. E., & Trower, E. J. (2020). Carbonate facies-specific stable isotope data record climate, hydrology, and microbial communities in Great Salt Lake, UT. *Geobiology*, 28. <https://doi.org/10.1111/gbi.12386>
- Jellison, R., & Melack, J. M. (2001). Nitrogen limitation and particulate elemental ratios of seston in hypersaline Mono Lake, California, U.S.A. In *Saline Lakes*. Springer.
https://doi.org/10.1007/978-94-017-2934-5_1
- Lemarchand, D., Wasserburg, G. J., & Papanastassiou, D. A. (2004). Rate-controlled calcium isotope fractionation in synthetic calcite. *Geochimica et Cosmochimica Acta*, 68(22), 4665–4678. <https://doi.org/10.1016/j.gca.2004.05.029>
- Nielsen, L. C., & DePaolo, D. J. (2013). Ca isotope fractionation in a high-alkalinity lake system: Mono Lake, California. *Geochimica et Cosmochimica Acta*, 118, 276–294.
<https://doi.org/10.1016/j.gca.2013.05.007>
- Nielsen, L. C., De Yoreo, J. J., & DePaolo, D. J. (2013). General model for calcite growth kinetics in the presence of impurity ions. *Geochimica et Cosmochimica Acta*, 115, 100–114.
<https://doi.org/10.1016/j.gca.2013.04.001>
- Ohno, T., & Zibilske, L. M. (1991). Determination of low concentrations of phosphorus in soil extracts using malachite green. *Soil Science Society of America Journal*.
<https://doi.org/10.2136/sssaj1991.03615995005500030046x>
- Ruttenberg, K. C., & Berner, R. A. (1993). Authigenic apatite formation and burial in sediments from non-upwelling, continental margin environments. *Geochimica et Cosmochimica Acta*, 57(5), 991–1007. [https://doi.org/10.1016/0016-7037\(93\)90035-U](https://doi.org/10.1016/0016-7037(93)90035-U)
- Saenger, C., Affek, H. P., Felis, T., Thiagarajan, N., Lough, J. M., & Holcomb, M. (2012). Carbonate clumped isotope variability in shallow water corals: Temperature dependence and growth-related vital effects. *Geochimica et Cosmochimica Acta*, 99, 224–242.
<https://doi.org/10.1016/j.gca.2012.09.035>
- Schneider, P., Hook, S. J., Radocinski, R. G., Corlett, G. K., Hulley, G. C., Schladow, S. G., & Steissberg, T. E. (2009). Satellite observations indicate rapid warming trend for lakes in California and Nevada. *Geophysical Research Letters*, 36(22), 1–6.
<https://doi.org/10.1029/2009GL040846>
- Smith, G. I. (1979). Subsurface stratigraphy and geochemistry of Late Quaternary evaporites, Searles Lake, California. *US Geological Survey, Professional Paper*, 1043, 130.

- 621 Spooner, P. T., Guo, W., Robinson, L. F., Thiagarajan, N., Hendry, K. R., Rosenheim, B. E., &
622 Leng, M. J. (2016). Clumped isotope composition of cold-water corals: A role for vital
623 effects? *Geochimica et Cosmochimica Acta*, 179, 123–141.
624 <https://doi.org/10.1016/j.gca.2016.01.023>
- 625 Thiagarajan, N., Crémière, A., Blättler, C., Lepland, A., Kirsimäe, K., Higgins, J., et al. (2020).
626 Stable and clumped isotope characterization of authigenic carbonates in methane cold seep
627 environments. *Geochimica et Cosmochimica Acta*, 279, 204–219.
628 <https://doi.org/10.1016/j.gca.2020.03.015>
- 629 Toner, J. D., & Catling, D. C. (2020). A carbonate-rich lake solution to the phosphate problem of
630 the origin of life. *Proceedings of the National Academy of Sciences of the United States of*
631 *America*, 117(2), 883–888. <https://doi.org/10.1073/pnas.1916109117>
- 632 Vasconcelos, C., & McKenzie, J. A. (1997). Microbial Mediation of Modern Dolomite
633 Precipitation and Diagenesis Under Anoxic Conditions (Lagoa Vermelha, Rio de Janeiro,
634 Brazil). *Journal of Sedimentary Research*. [https://doi.org/10.1306/D4268577-2B26-11D7-](https://doi.org/10.1306/D4268577-2B26-11D7-8648000102C1865D)
635 [8648000102C1865D](https://doi.org/10.1306/D4268577-2B26-11D7-8648000102C1865D)
- 636 Van Veldhoven, P. P., & Mannaerts, G. P. (1987). Inorganic and organic phosphate
637 measurements in the nanomolar range. *Analytical Biochemistry*.
638 [https://doi.org/10.1016/0003-2697\(87\)90649-X](https://doi.org/10.1016/0003-2697(87)90649-X)
- 639 Watkins, J. M., & Hunt, J. D. (2015). A process-based model for non-equilibrium clumped
640 isotope effects in carbonates. *Earth and Planetary Science Letters*, 432.
641 <https://doi.org/10.1016/j.epsl.2015.09.042>
- 642 Whitman, W. B., Coleman, D. C., & Wiebe, W. J. (1998). Prokaryotes: The unseen majority.
643 *Proceedings of the National Academy of Sciences of the United States of America*.
644 <https://doi.org/10.1073/pnas.95.12.6578>